

A study and Analysis of CNN approach for the Lung Cancer Detection Using Deep Domain Adaption Technique and Image Processing

¹Dr. Sheetanshu Rajoriya, Supervisor, Sunrise University, Alwar

²Pramod Kumar Sharma, Scholar, Sunrise University, Alwar

Abstract

Medical imaging provides non-invasive assessments of phenotypic diversities in a number of cancer types. Medical images have the potential to offer insights into the patterns of disease spread and treatment response. Furthermore, advances in computerized medical image analysis enable the extraction of tumor's visual representation (features) to facilitate characterizing tumour phenotypes. The association between tumor imaging biomarkers and existing genetic foreknowledge lead to the emergence of image-genomics.

In this paper we review a deep domain adaptation learning framework for associating image features to tumour genetic information. Our approach exploits the potential of domain adaptation technique for image-genomics to quantify image features based on similar knowledge domains. This is accomplished by facilitating the learning of tumour image representations with larger datasets from similar domains to reduce the reliance on large volumes of disease-specific datasets for image-genomics research.

In addition, our proposed framework enables the extraction of additional tumour visual descriptors to provide abstract image representations for associating with gene expressions. It leverages the current state-of-the-art in image object recognition to provide image features which encode subtle variations of tumour phenotypic characteristics. The quantification of such features is facilitated by the employment of domain adaptation techniques. We evaluated our proposed deep domain adaptation learning framework by comparing with current state-of-the-art in: (i) tumour histopathology image classification and; (ii) the degree of image-genomics associations compare with human-crafted tumour image descriptors.

Keywords: Cancer Detection, Image processing, CNN, Machine Learning, Deep learning.

Introduction

Current practices for the treatment of human cancers rely upon the establishment of accurate diagnosis, which may involve a series of complex medical procedures comprising of patient screening for symptom evaluation, non-invasive imaging for disease localization and histopathology analysis of tissue specimens. In recent years, genetic sequencing is becoming an increasingly important addition to the existing diagnostic pipeline. Cancer diagnosis may be the result of analysis of data generated through each medical examinations; the integration of such data contributes towards the understanding of the diseases and hence exhibit potentials to offer optimal cancer therapy at individual patient level [1]. Although medical imaging and general pathology are becoming more routine in current cancer diagnosis, genetic sequencing is not always practical. This is due to human cancers exhibits strong phenotypic and genetic heterogeneity, where disease develops at multiple sites with genetic differences [2]. It is not practical or feasible to obtain tissue samples

from all sites of disease as invasive biopsies have the potential to induce tumor proliferation. Further, the cost of genetic examination is high in addition to its limited accessibility.

As an alternative, medical images provide non-invasive assessments of phenotypic diversities in a number of cancer types and contribute to clinical decision-making, e.g., tumor detection, subtype characterization and treatment responses [3, 4]. Advances in computerized medical image analysis allow the extraction of tumor's visual representations (features) to facilitate the characterization of tumor phenotypic differences, which offers insights into the patterns of disease spread and prognosis. The association between tumor imaging features and genetic foreknowledge allows the derivation of imaging surrogates to genetic biomarkers, and ultimately lead to the emerging field of image-genomics [5].

Image-genomics aims to associate the tumor imaging trait and clinical data (e.g., the underlying tumor gene expression) to provide an alternative approach that contributes to a non-invasive and accurate cancer diagnosis [6]. As such, the discovery and extraction of optimized tumor imaging descriptors represent a major challenge in the current image-genomics research.

Medical Imaging and Image Processing

A Medical imaging is a fundamental component of the modern healthcare system and is essential for the accurate diagnosis and staging of cancers. Medical images provide a fast and non-invasive assessment of phenotypic diversity in many cancers [12] through a variety of different imaging modalities (or techniques). Medical image processing, in turn, allows the extraction of meaningful information which offers insights of different aspects of patients' conditions. In this chapter, we provide an overview of medical imaging and the theoretical background in image processing techniques that are crucial for cancer diagnosis.

Digital images consist of a collection of numerical picture elements, called pixels. The term pixel resolution refers to the number of pixels in an image, which can be represented as a single number or by the number of pixels in each dimension. For example, an image that contains 8,294,400 pixels can also be referred to as having a resolution of 8.3 megapixels or 3840×2160 (width \times height) pixels.

Many medical imaging techniques consist of sampling 2D images along a third spatial axis to form 3D images, known as volumetric images or image volumes. These 3D volumetric images encode the spatial relationships between 3D pixels, called voxels, which both 2D and 3D images allow the extraction and interpretation of the encoded information through the use of image processing techniques. Both pixels and voxels exhibit spatial resolutions, which describe the size of the details captured by individual pixels or voxels. For instance, a spatial resolution of $10.00\text{mm} \times 10.00\text{mm} \times 5.00\text{mm}$ means that a voxel depicts a region with a volume of 500.00 mm^3 .

Contrast resolution refers to the range of distinct intensity or a set of intensities for red, green and blue (RGB) channels that can be distinguished in grayscale and colored images respectively. A relatively low contrast resolution can be interpreted as pixel/voxel intensities that are similar in an image and are difficult to distinguish.

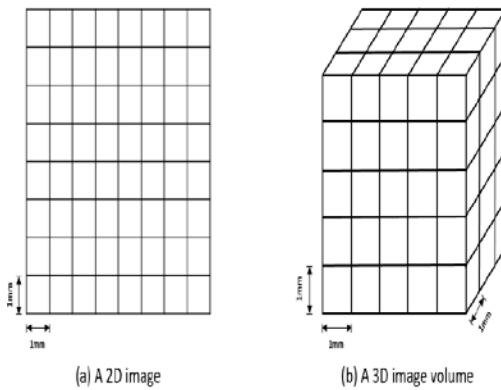


Fig 1 : illustrates an example of a 2D image and a 3D volumetric image. Pixels and voxels are visualized in forms of 2D and 3D arrays of grids respectively

In medical image processing, a region of interest (ROI) consists collections of pixels in 2D images that represent an area which encodes important information for particular domain or application in cancer diagnosis. The corresponding term volume of interest (VOI) refers to the emphasized anatomical structures that encode important knowledge for clinical uses.

Modern healthcare utilizes different medical imaging modalities to capture different aspects of the human body for cancer diagnostic and treatment. Medical image modalities can be categorized into two classes based on their technique and process in visualizing different aspects of the diseases: (i) Anatomical and (ii) Physiological (functional) imaging. Anatomical medical images capture and visualize the anatomical structures of the ROI in the form of 2D or 3D images. Anatomical medical images allow physicians to interpret and evaluate the disease conditions for diagnosis purposes, and can also be used for the monitoring of treatment responses [4]. Functional imaging, on the other hand, captures the metabolic status of the ROI, which allows physicians to assess the physiological status of patients, and to identify structures with abnormalities, such as tumors.

Common anatomical medical image modalities include X-ray, computed tomography (CT), magnetic resonance imaging (MRI). Common functional imaging includes single-photon emission computed tomography (SPECT) and positron emission tomography (PET). Such image techniques produce a single type of image or image volumes that are referred as single-modality medical imaging.

Similar to CT images, digital WSI enables medical image analysis techniques to be applied to extract image features of abnormal cells. Image traits can then be exploited to correlate to genetic profiles of the tumor.

Methodology

Machine learning techniques for medical image processing are a well-established field. The ability of machine learning to quantify the representation features of the input medical image empowers numerous automated medical image processing algorithms for different clinical applications. However, machine learning systems were limited due to its requirement of domain expertise with careful engineering to be able to learn and transform the input data. Deep learning is a class of machine learning technique which allows learning of data representations with multiple layers of abstraction. Convolution

neural networks (CNNs) are a deep learning technique that extracts image features from imaging data to learn the sophisticated underlying representations with deep networks.

Machine Learning

Machine learning is a major field of computer science that has been utilized to serve many aspects of modern healthcare systems. With carefully engineered mathematical models, machine-learning systems have been applied in pattern recognition, image classification, medical image retrieval and tumor image segmentation. Compare to the rule-based systems, the core of machine learning techniques are based on the development of models from statistical and artificial intelligence approaches. It is essential for the machine learning model to “learn” to recognize the distinguishing characteristics of the patterns within the data to produce meaningful outputs. Generally, the learning approaches for machine learning models are divided into the following: supervised learning, unsupervised learning and reinforcement learning.

Although unsupervised and reinforcement learning exhibit strong potentials in multiple disciplines, our contribution rely on labeled medical imaging data to explore the region-specific genetic association. As the contributions of this thesis involve mainly supervised approaches, we will only cover those approaches here. Supervised training approaches require several different types of database, defined as follows:

Training data: refers to a collection of data that are used to train the machine learning model. The machine learning model learns the representation of the training data and its predictive relationship to the output labels. **Validation data:** refers to a separate collection of data that are used in addition to the training data to adjust or guide the training process. This process involves the comparison between the predicted output with the training data labels. This provides an indication of the performance of the model on unseen data during the training process, and allows tuning of model parameters.

Test data: refers to a collection of withheld data which is used to evaluate the performance of the model at the after the completion of the training process. Test data indicates the performance of the trained model with new examples. Test data are not involved in the training process.

Supervised Learning

Supervised learning is one of the most common approaches for medical image processing and analysis. It refers to the approach where the model is trained with labeled data sets so that the model learns the internal representation of the input data to make predictions on the labels [13]. The resulting model from supervised learning is typically used to assign class labels with known predictive features for future data sets. Supervised learning is capable of performing classification or regression with training data set with discrete or continuous properties, respectively.

Artificial Neural Network

Artificial Neural Networks (ANNs) are a machine learning approach that was inspired by the biological neural networks that constitute human brains [20]. An ANN consists a collection of connected nodes or “artificial neurons” in a directed graph in the form of networks. ANNs are commonly used in machine learning to learn the complex non-linear relationships from the dataset. This is achieved through the ANN’s mechanisms where each neuron receives, processes and transmits a signal from one to another in a similar way to the biological synapse. To achieve the optimized learning

outcome, ANN requires the design of an appropriate network structure and learning approach to tune the weights and biases of the network.

Neurons are the fundamental building blocks of many ANNs. Fig 2 illustrates the structure of a single neuron where multiple inputs values are processed in the neuron to produce a single output value, where X is a vector of inputs with n elements, W is the vector of the weights with a corresponding number of elements.

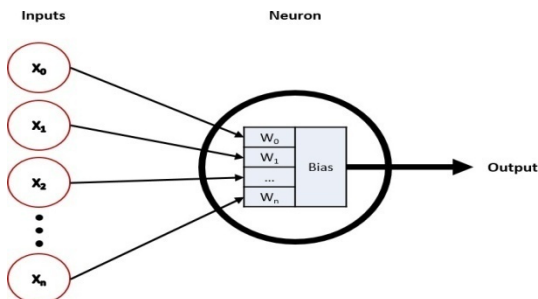


Fig 2: Representation of a single model neuron

The training of an ANN can be explained by illustrated single neuron model. For each element in the training dataset, its features are extracted and transmitted into the neuron in the form of a feature vector. Assuming that the classification task involves only two classes, the neuron processes the input feature vector by multiplying with its internal weights. A class prediction is based on whether the value of the product is above a threshold. If the predicted class does not match the corresponding label, each weight within the neuron is adjusted individually to refine the prediction process. Additionally, the training dataset is typically divided into collections of batches which allows the weight adjustment after training of each batch. An epoch refers to the full pass of the entire training dataset; robust weights for classification tasks are the outcome of hundreds of training epochs.

Deep Learning

Deep learning can be categorized as a class of techniques of machine learning, which allows the computation models with multiple processing layers to learn the internal representation of the input data with multiple levels of abstraction. Deep learning was proposed to address the limited performance of traditional machine learning approaches to process natural data in their raw form. Deep learning resolves this issue by utilizing the multiple processing layers to learn and interpret the low level, abstract representations from the high-level understandings of the input dataset [12]. This is achieved by feeding the raw data through the successive multilayer architecture in a sequential manner, where deeper layers learn the abstract representation from the representation in the previous layers.

Deep learning technique employs backward propagation of error or “back propagation” to train the multilayer model for supervised learning [11]. Back propagation calculates the gradient of the error function of the ANN with respect to its weights and passes the gradient backwards through the neural network. Compared to the traditional approach where the gradient of the error function is calculated for each layer separately, the backflow of error gradient allows more efficient computation of gradient for ANNs.

The implementation of deep learning technique utilizes specialized GPUs to improve the performance of training process by 10 to 20 times compared to the traditional training approach on standard CPUs. Recent advances in deep learning have

lead to the improved state-of-the-art in various domains such as visual object recognition, speech recognition and also in medical image analysis.

Convolutional Neural Networks

Convolutional Neural Networks (CNNs) is a particular type of ANN and designed to process input data that is in the form of multidimensional arrays, e.g., colored 2D images which consist of 2D arrays for each RGB (color) channel. Compared with traditional ANNs with fully connected adjacent layers, CNNs are much easier to train and are more generalized. CNNs are structured in a series of stages where each stage consists of specialized layers with unique functions. The building blocks of a CNN consists three types of specialized layers: Convolution, pooling and activation layers, e.g., rectified linear unit (ReLU) layers.

Convolution layers consist of organized units in the form of feature maps, where each unit is connected to local patches from the previous layer through a set of weights which is referred as filter. This design allows the Convolution layers to detect local conjunctions of features from the previous layer, as local values are often highly correlated and are invariant to the location in an image input.

Pooling layers are designed to merge features in spatial proximity which share semantic similarities into one. The principle behind pooling layers is to detect the position of motifs that are typically formed by highly correlated features through a coarse-grained approach. An example pooling layer calculates the maximum of a local patch in one or more feature maps. Pooling layers act to reduce the dimensions of the representations and to create an invariance to small distortions and shifts.

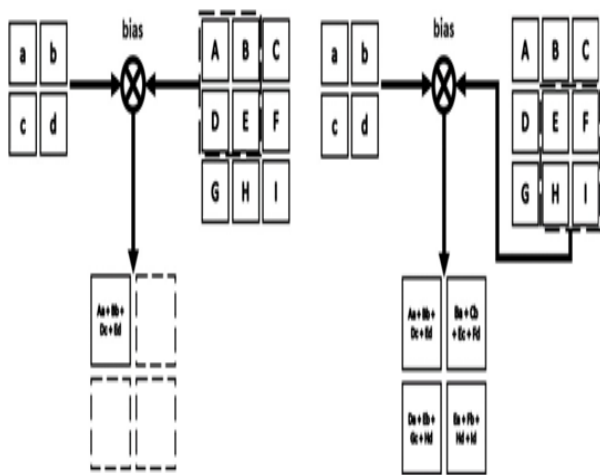


Fig 3: An example 2D convolution of a 3×3 input using a 2×2 filter with the 2×2 output feature map

Results

Results demonstrated that domain adaptation technique facilitates the learning of image representations of abnormalities in medical images by extending or refining existing knowledge from similar domains. The quantification of such image features hence improves the accuracy of tumor image classification tasks, compared to traditional approaches where deep learning models were trained from scratch on limited volumes of domain-specific datasets. Our results also demonstrated that the proposed framework offers additional deep image features to encode abstract representation of tumor phenotypic

characteristics which exhibit stronger associations to patient-specific genetic information, compared to human-crafted image features.

Domain adaptation is the ability to apply an algorithm trained in one or more "source domains" to a different (but related) "target domain". Domain adaptation is a subcategory of transfer learning. In domain adaptation, the source and target domains all have the same features space (but different distributions); in contrast, transfer learning includes cases where the target domain's feature space is different from the source feature space or spaces.

Conclusion

In this paper, we presented novel deep domain adaptation learning framework for image-genomics analysis to improve image-genomics association. Our proposed framework emphasized the employment of domain adaptation of deep learning in image-genomics research to offer additional deep image features that encode abstract image representations of subtle variation in tumor medical images. Our domain adaptation approach reduces the dependency on large volumes of annotated medical image dataset for deep learning models to learn the tumor image representation.

References

1. Kumar, Rajesh "A novel multi-objective directed bee colony optimization algorithm for multi-objective emission constrained economic power dispatch." *International Journal of Electrical Power & Energy Systems*, pp-1241-1250, 2012.
2. Raglend, I. Jacob, et al. "Comparison of AI techniques to solve combined economic emission dispatch problem with line flow constraints." *International Journal of Electrical Power & Energy Systems*, pp-592-598, 2010.
3. C. R. King, "Patterns of prostate cancer biopsy grading: trends and clinical implications," *International journal of cancer*, vol. 90, pp. 305-311, 2000.
4. B. L. Baisden, H. Kahane, and J. I. Epstein, "Perineural invasion, mucinous fibroplasia, and glomerulations: diagnostic features of limited cancer on prostate needle biopsy," *The American journal of surgical pathology*, vol. 23, p. 918, 1999
5. B. Bain, "Bone marrow biopsy morbidity and mortality: 2002 data," *International Journal of Laboratory Hematology*, vol. 26, pp. 315-318, 2004
6. H. Su, Y. Shen, F. Xing, X. Qi, K. M. Hirshfield, L. Yang, et al., "Robust automatic breast cancer staging using a combination of functional genomics and image-omics," in *Engineering in Medicine and Biology Society (EMBC), 2015 37th Annual International Conference of the IEEE, 2015*, pp. 7226- 7229.
7. Madabhushi and G. Lee, "Image analysis and machine learning in digital pathology: Challenges and opportunities," *Medical image analysis*, vol. 33, pp. 170-175, 2016.

8. H. J. Aerts, E. R. Velazquez, R. T. Leijenaar, C. Parmar, P. Grossmann, S. Cavalho, et al., "Decoding tumour phenotype by noninvasive imaging using a quantitative radiomics approach," *Nature communications*, vol. 5, 2014.
9. O. Gevaert, J. Xu, C. D. Hoang, A. N. Leung, Y. Xu, A. Quon, et al., "Non-small cell lung cancer: identifying prognostic imaging biomarkers by leveraging public gene expression microarray data—methods and preliminary results," *Radiology*, vol. 264, pp. 387-396, 2012.
10. S. Banerjee, D. S. Wang, H. J. Kim, C. B. Sirlin, M. G. Chan, R. L. Korn, et al., "A computed tomography radiogenomic biomarker predicts microvascular invasion and clinical outcomes in hepatocellular carcinoma," *Hepatology*, vol. 62, pp. 792-800, 2015.
11. M. D. Kuo, J. Gollub, C. B. Sirlin, C. Ooi, and X. Chen, "Radiogenomic analysis to identify imaging phenotypes associated with drug response gene expression programs in hepatocellular carcinoma," *Journal of Vascular and Interventional Radiology*, vol. 18, pp. 821-830, 2007.
12. Y. Bengio, "Learning deep architectures for AI," *Foundations and trends® in Machine Learning*, vol. 2, pp. 1-127, 2009.
13. S. Rosenstein, C. M. West, S. M. Bentzen, J. Alsner, C. N. Andreassen, D. Azria, et al., "Radiogenomics: radiobiology enters the era of big data and team science," *International Journal of Radiation Oncology• Biology• Physics*, vol. 89, pp. 709-713, 2014.
14. S. Takhar, P. Palaniappan, R. Dhingsa, and D. N. Lobo, "Recent developments in diagnosis of pancreatic cancer," *BMJ: British Medical Journal*, vol. 329, p. 668, 2004.
15. K. Horsthuis, P. C. Stokkers, and J. Stoker, "Detection of inflammatory bowel disease: diagnostic performance of cross-sectional imaging modalities," *Abdominal imaging*, vol. 33, pp. 407-416, 2008.
16. W. Townsend and S. R. Cherry, "Combining anatomy and function: the path to true image fusion," *European radiology*, vol. 11, pp. 1968-1974, 2001.
17. R. D. Pascual-Marqui, M. Esslen, K. Kochi, and D. Lehmann, "Functional imaging with low-resolution brain electromagnetic tomography (LORETA): a review," *Methods and findings in experimental and clinical pharmacology*, vol. 24, pp. 91-95, 2002.
18. H. Fischer, K. A. Jacobson, J. Rose, and R. Zeller, "Hematoxylin and eosin staining of tissue and cell sections," *Cold Spring Harbor Protocols*, vol. 2008, p. pdb. prot4986, 2008.
19. M. J. Reardon, J.-C. Walkes, and R. Benjamin, "Therapy insight: malignant primary cardiac tumors," *Nature Reviews Cardiology*, vol. 3, p. 548, 2006.
20. S. Kothari, J. H. Phan, T. H. Stokes, and M. D. Wang, "Pathology imaging informatics for quantitative analysis of whole-slide images," *Journal of the American Medical Informatics Association*, vol. 20, pp. 1099-1108, 2013.

21. L. Pham, C. Xu, and J. L. Prince, "Current methods in medical image segmentation," Annual review of biomedical engineering, vol. 2, pp. 315-337, 2000.
22. R. A. Poldrack, "Region of interest analysis for fMRI," Social Cognitive and Affective Neuroscience, vol. 2, pp. 67-70, March 1, 2007

Review paper on Analysis of CNN approach for Lung Cancer Detection and Classification
¹Dr. Sheetanshu Rajoriya, Supervisor, Sunrise University, Alwar

²Pramod Kumar Sharma, Scholar, Sunrise University, Alwar

Abstract

This paper shows a computer-aided diagnostic (CAD) method, a dataset from the for lung cancer classification of CT scans with unmarked nodules. As an initial segmentation approach, thresholding was used to segment out lung tissue from the remainder of the CT scan. The next finest lung segmentation was created by Thresholding. The initial solution was to feed the segmented CT scans directly for classification into 3D CNNs, but this proved to be insufficient. Instead, the first identification of nodule candidates in the CT scans was performed by an updated U-Net trained on LUNA16 data (CT scans with labelled nodules). In order to identify the CT scan as positive or negative for lung cancer, the U-Net nodule detection provided several false positives, so regions of CTs with segmented lungs where the most likely nodule candidates were located as defined by the U-Net production were fed into 3D Convolutional Neural Networks (CNNs). The 3D CNNs provided the Accuracy O Test Set. Our CAD system's efficiency outperforms the existing literature CAD systems that have many preparation and testing levels, each involving a lot of labelled data, whereas our CAD system has only three key stages (segmentation, nodule candidate identification, and classification of malignancy), allowing more effective training and detection and more generalization for other cancers

Keywords: Lung cancer; computed tomography; deep learning; Convolutional neural networks; segmentation

Introduction

Lung cancer is one of the most prevalent diseases responsible for over 225,000 cases, 150,000 deaths, and \$12 billion in total health care expenses. It is also one of the worst cancers; nationally, only 17 percent of people diagnosed with lung cancer in the country live five years after diagnosis, although in developed countries, the mortality rate is smaller. A cancer's level corresponds to how deeply it has metastasized. Stages 1 and 2 refer to cancers found in the lungs, and cancers that have spread to other organs refer to the later stages. Present screening procedures, such as CT scans, include biopsies and imaging. Early diagnosis of lung cancer (detection during the earlier stages) greatly increases the probability of survival, but early detection of lung cancer is often more difficult when less symptoms are present. [1].

In patient CT scans of lungs with and without early stage lung cancer, our job is a binary classification question to diagnose the existence of lung cancer. To create an accurate classifier, we aim to use techniques from computer vision and deep learning, particularly 2D and 3D convolutionary neural networks. An correct classification of lung cancer could accelerate and reduce the cost of screening for lung cancer, encouraging more universal screening.

Early identification and survival change. The aim is to build a computer-aided diagnostic (CAD) system that involves patient chest CT scans and outputs as an input, whether the patient has lung cancer or not. [2].

Although this job sounds simple, in the haystack dilemma it is really a needle. The CAD device will have to detect the presence of a small nodule (< 10 mm in diameter for early stage cancers) from a large 3D lung CT scan to determine whether or not a patient has early-stage cancer (typically around 200 mm 400 mm 400 mm). An example of an early stage

nodules of lung cancer seen in a 2D slice of a CT scan is given in Fig. 1. In addition, a CT scan is packed with noise from nearby tissues, bone, air, so this noise will first have to be preprocessed for the CAD systems search to be successful. Therefore, image preprocessing, nodule candidate identification, malignancy classification are our classification pipeline. In this article, we use systematic preprocessing procedures to extract specific nodules in order to increase the precision of lung cancer diagnosis. In addition, we conduct CNN end-to-end testing from scratch in order to understand the full capacity of the neural network, i.e. to acquire discriminatory characteristics. A dataset containing lung nodules from more than 1390 low dose CT scans is used for detailed experimental assessments.

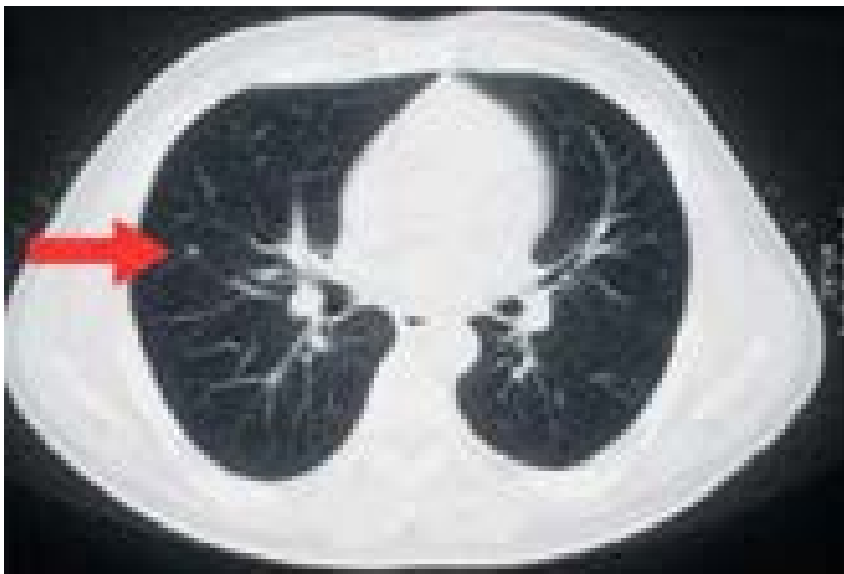


Figure 1: 2D CT scan slice containing a small (5mm) early stage lung cancer nodule.

Related Work

Recently, deep artificial neural networks have been applied in many applications in pattern recognition and machine learning, especially, Convolutional neural networks (CNNs) which is one class of models [3]. Another approach of CNNs was applied on ImageNet Classification in 2012 is called an ensemble CNNs which outperformed the best results which were popular in the computer vision community [4]. There has also been popular latest research in the area of medical imaging using deep learning with promising results.

R. Golan proposed a framework that trains the weights of the CNN by a back propagation to detect lung nodules in the CT image sub-volumes. This system achieved sensitivity of 78.9% with 20 false positives, while 71.2% with 10 FPs per scan, on lung nodules that have been annotated by all four radiologists.

Convolutional neural networks have achieved better than Deep Belief Networks in current studies on benchmark computer vision datasets. The CNNs have attracted considerable interest in machine learning since they have strong representation ability in learning useful features from input data in recent years.

Data

Our primary dataset is the patient lung CT scan dataset from Cancer Hospital. The dataset contains labeled data for 1475 patients, which we divide into training set of size 900, and test set of size 575. For each patient, the data consists of CT scan data and a label (0 for no cancer, 1 for cancer). Note that the dataset does not have labeled nodules. For each

patient, the CT scan data consists of a variable number of images (typically around 100- 400, each image is an axial slice) of 512 × 512 pixels. The slices are provided in DICOM format. Around 70% of the provided labels in the dataset are 0, so we used a weighted loss function in our malignancy classifier to address this imbalance.

Dataset alone proved to be inadequate to accurately classify the validation set, we also used the patient lung CT scan dataset with labeled nodules from the Lung Nodule Analysis 2016 (LUNA16) Challenge to train a U-Net for lung nodule detection. The LUNA16 dataset contains labeled data for 888 patients, which we divided into a training set of size 710 and a validation set of size 178. For each patient, the data consists of CT scan data and a nodule label (list of nodule center coordinates and diameter). For each patient, the CT scan data consists of a variable number of images (typically around 100-400, each image is an axial slice) of 512 × 512 pixels. LUNA16 data was used to train a U-Net for nodule detection, one of the phases in our classification pipeline. The problem is to accurately predict a patient’s label (‘cancer’ or ‘no cancer’) based on the patient’s Kaggle lung CT scan. We will use accuracy, sensitivity, specificity, and AUC of the ROC to evaluate our CAD system’s performance on the test set.

Methods

Typical CAD systems for lung cancer have the following pipeline: image preprocessing, detection of cancerous nodule candidates, nodule candidate false positive reduction, malignancy prediction for each nodule candidate, and malignancy prediction for overall CT scan [15]. These pipelines have many phases, each of which are computationally expensive and require well-labeled data during training. For example, the false positive reduction phase requires a dataset of labeled true and false nodule candidates, and the nodule malignancy prediction phase requires a dataset with nodules labeled with malignancy.

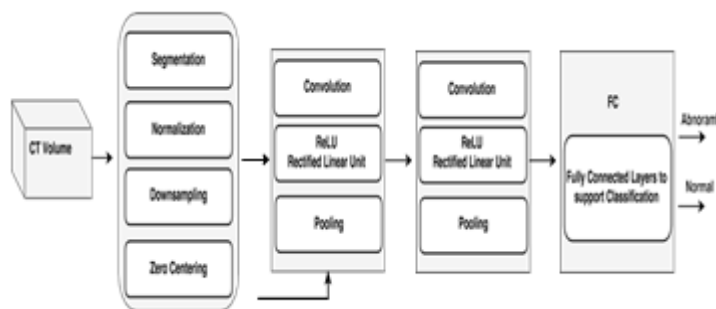


Figure 2: 3D Convolutional neural networks architecture

True/False labels for nodule candidates and malignancy labels for nodules are sparse for lung cancer, and may be nonexistent for some other cancers, so CAD systems that rely on such data would not generalize to other cancers. In order to achieve greater computational efficiency and generalizability to other cancers, the proposed CAD system has shorter pipeline and only requires the following data during training: a dataset of CT scans with true nodules labeled, and a dataset of CT scans with an overall malignancy label. State-of-the-art CAD systems that predict malignancy from CT scans achieve AUC of up to 0.83 [16]. However, as mentioned above, these systems take as input various labeled data that is not used in this framework. The main goal of the proposed system is to reach close to this performance.

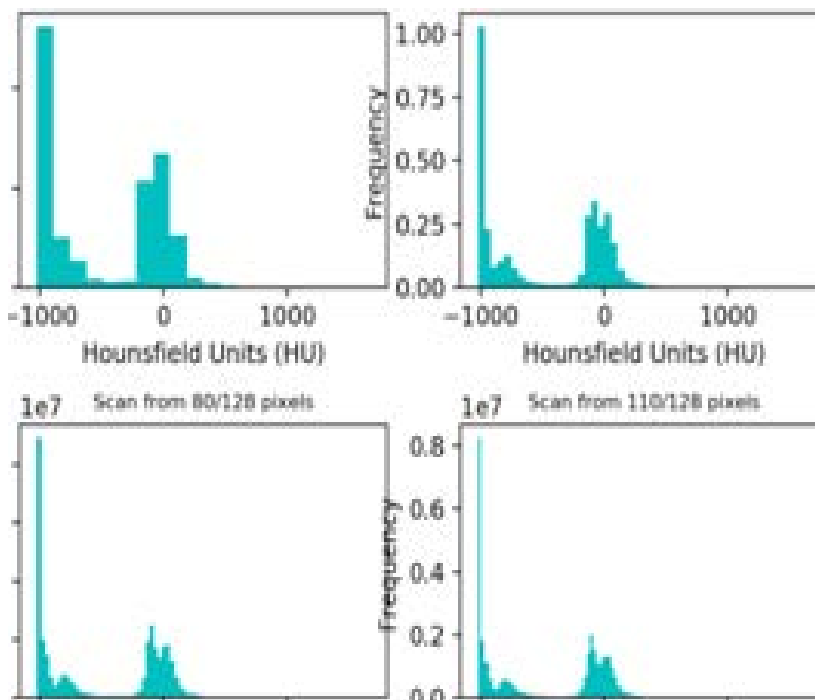
The proposed CAD system starts with preprocessing the 3D CT scans using segmentation, normalization, down sampling, and zero-centering. The initial approach was to simply input the preprocessed 3D CT scans into 3D CNNs, but the results

were poor. So an additional preprocessing was performed to input only regions of interests into the 3D CNNs. To identify regions of interest, a U-Net was trained for nodule candidate detection. Then input regions around nodule candidates detected by the U-Net was fed into 3D CNNs to ultimately classify the CT scans as positive or negative for lung cancer. The overall architecture is shown in Fig. 2, all details of layers will be described in the next sections.

A. Preprocessing and Segmentation

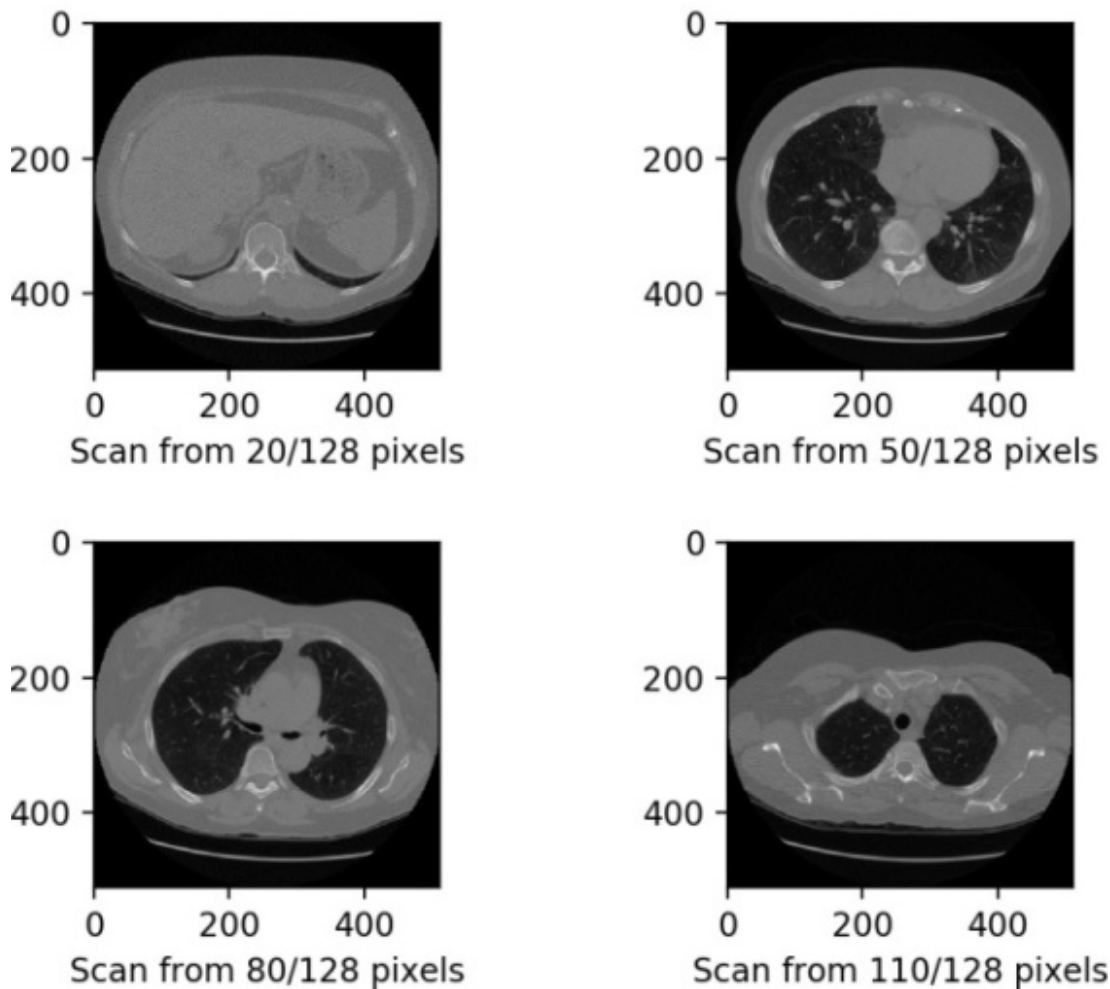
For each patient, pixel values was first converted in each image to Hounsfield units (HU), a measurement of radio density, and 2D slices are stacked into a single 3D image. Because tumors form on lung tissue, segmentation is used to mask out the bone, outside air, and other substances that would make data noisy, and leave only lung tissue information for the classifier. A number of segmentation approaches were tried, including thresholding, clustering (Kmeans and Meanshift), and Watershed. K-means and Meanshift allow very little supervision and did not produce good qualitative results. Watershed produced the best qualitative results, but took too long to run to use by the deadline. Ultimately, thresholding was used.

After segmentation, the 3D image is normalized by applying the linear scaling to squeeze all pixels of the original unsegmented image to values between 0 and 1. Spline interpolation down samples each 3D image by a scale of 0.5 in each of the three dimensions. Finally, zero-centering is performed on data by subtracting the mean of all the images from the training set.



(a).Histograms of pixel values in HU for sample patients CT scan at various slices.

Scans from different locations for one patient



(b). Corresponding 2D axial slices.

Figure 3: Histogram of HU values at 3b corresponding axial slices for sample patient 3D image at various axial.

Simulation Results

The experiments are conducted using DSB dataset. In this dataset, a thousand low-dose CT images from high-risk patients in DICOM format is given. The DSB database consists of 1397 CT scans and 248580 slices. Each scan contains a series with multiple axial slices of the chest cavity. Each scan has a variable number of 2D slices (Fig. 4), which can vary based on the machine taking the scan and patient. The DICOM files have a header that contains the necessary information about the patient id, as well as scan parameters such as the slice thickness. It is publicly available in the . Dicom is the de-facto file standard in medical imaging. This pixel size/coarseness of the scan differs from scan to scan (e.g. the distance between slices may differ), which can hurt performance of our model.

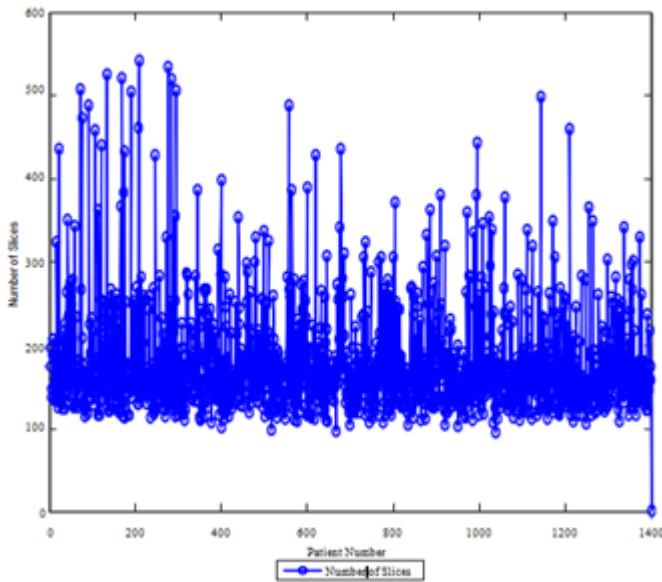


Figure 4: Number of slices per patient in data science bowl dataset.

The accuracy metric is the used metric in our evaluations. In our first set of experiments we considered a range of CNN architectures for the binary classification task. Early experimentation suggested that the number of filters and neurons per layer were less significant than the number of layers. Thus, to simplify analysis the first Convolutional layer used seven filters with size 5 5 5, the second Convolutional layer used 17 filters with 5 5 3 and all fully connected layers used 256 neurons. These were found to generally perform well and we considered the impact of one or two Convolutional layers followed by one or two fully connected layers. The networks were trained as described above and the results of these experiments can be found in Table I. Our results suggest that two Convolutional layers followed by a single hidden layer is one of the optimal network architecture for this dataset. The average error for training .

Another important parameter in the training of neural networks is the number of observations that are sampled at each iteration, the size of the so-called mini batch.

The use of mini batches is often driven in part by computational considerations but can impact the ability of SGD to find a good solution. Indeed, we found that choosing the proper mini batch size was critical for learning to be effective. We tried mini batches of size 1, 10, 50 and 100. While the nature of SGD suggests that larger batch sizes should produce better gradient estimates and there for work better, our results here show that the opposite is true. Smaller batch sizes, even as small as 1, produce the best results. We suspect that the added noise of smaller batch sizes allows SGD to better escape poor local optima and thus perform better overall.

The recognition results are shown by confusion matrix achieved on the DSB dataset with 3D CNN as shown in Table As shown from the Table, Accuracy of model is 86.6%, Misclassification rate is 13.4%, False positive rate is 11.9%, and False Negative is 14.7%. Almost all patients are classified correctly. Additionally, there is an enhancement on accuracy due to efficient U-Net architecture and segmentation.

Actual	Abnormal	Normal
Abnormal	0.853	0.147
Normal	0.119	0.881

Table I: Confusion Matrix of 3D CNN using 30% Testing

Conclusion

In this paper, discussed a deep Convolutional neural network (CNN) architecture to detect nodules in patients of lung cancer and detect the interest points using U-Net architecture. This step is a preprocessing step for 3D CNN. The deep 3D CNN models performed the best on the test set. While we achieve state-of-the-art performance AUC of 0.83, we perform well considering that we use less labeled data than most state-of-the-art CAD systems. As an interesting observation, The first layer is a preprocessing layer for segmentation using different techniques. Threshold, Watershed, and U-Net are used to identify the nodules of patients.

The network can be trained end-to-end from raw image patches. Its main requirement is the availability of training database, but otherwise no assumptions are made about the objects of interest or underlying image modality.

In the future, it could be possible to extend our current model to not only determine whether or not the patient has cancer, but also determine the exact location of the cancerous nodules. The most immediate future work is to use Watershed segmentation as the initial lung segmentation. Other opportunities for improvement include making the network deeper, and more extensive hyper parameter tuning. Also, we saved our model parameters at best accuracy, but perhaps we could have saved at other metrics, such as F1. Other future work include extending our models to 3D images for other cancers. The advantage of not requiring too much labeled data specific to our cancer is it could make it generalizable to other cancers.

References

1. W.-J. Choi and T.-S. Choi, “Automated pulmonary nodule detection system in computed tomography images: A hierarchical block classification approach,” *Entropy*, vol. 15, no. 2, pp. 507–523, 2013.
2. A. Chon, N. Balachandar, and P. Lu, “Deep Convolutional neural networks for lung cancer detection,” tech. rep., Stanford University, 2017.
3. Y. LeCun, K. Kavukcuoglu, and C. Farabet, “Convolutional networks and applications in vision.,” in *Proceedings of the IEEE International Symposium on Circuits and Systems (ISCAS)*, pp. 253–256, IEEE, 2010.
4. K. Alex, I. Sutskever, and G. E. Hinton, “Imagenet classification with deep convolutional neural networks,” in *Advances in Neural Information Processing Systems 25 (NIPS 2012)* (F. Pereira, C. J. C. Burges, L. Bottou, and K. Q. Weinberger, eds.), pp. 1097–1105, 2012.
5. H. Suk, S. Lee, and D. Shen, “Hierarchical feature representation and multimodal fusion with deep learning for AD/MCI diagnosis,” *NeuroImage*, vol. 101, pp. 569–582, 2014.
6. G. Wu, M. Kim, Q. Wang, Y. Gao, S. Liao, and D. Shen, “Unsupervised deep feature learning for deformable registration of mr brain images.,” *Medical Image Computing and Computer-Assisted Intervention*, vol. 16, no. Pt 2, pp. 649–656, 2013.

7. Y. Xu, T. Mo, Q. Feng, P. Zhong, M. Lai, and E. I. Chang, "Deep learning of feature representation with multiple instance learning for medical image analysis," in *IEEE International Conference on Acoustics, Speech and Signal Processing, ICASSP*, pp. 1626–1630, 2014.
8. D. Kumar, A. Wong, and D. A. Clausi, "Lung nodule classification using deep features in ct images," in *2015 12th Conference on Computer and Robot Vision*, pp. 133–138, June 2015.
9. Y. Bar, I. Diamant, L. Wolf, S. Lieberman, E. Konen, and H. Greenspan, "Chest pathology detection using deep learning with non-medical training," *Proceedings - International Symposium on Biomedical Imaging*, vol. 2015-July, pp. 294–297, 2015.
10. W. Sun, B. Zheng, and W. Qian, "Computer aided lung cancer diagnosis with deep learning algorithms," in *SPIE Medical Imaging*, vol. 9785, pp. 97850Z–97850Z, International Society for Optics and Photonics, 2016.
11. J. Tan, Y. Huo, Z. Liang, and L. Li, "A comparison study on the effect of false positive reduction in deep learning based detection for juxtapleural lung nodules: Cnn vs dnn," in *Proceedings of the Symposium on Modeling and Simulation in Medicine, MSM '17*, (San Diego, CA, USA), pp. 8:1–8:8, Society for Computer Simulation International, 2017.
12. R. Golan, C. Jacob, and J. Denzinger, "Lung nodule detection in ct images using deep Convolutional neural networks," in *2016 International Joint Conference on Neural Networks (IJCNN)*, pp. 243–250, July 2016.
13. Kaggle, "Data science bowl 2017." <https://www.kaggle.com/c/data-science-bowl-2017/data>, 2017.
14. LUNA16, "Lung nodule analysis 2016." <https://luna16.grand-challenge.org/>, 2017.
15. M. Firmino, A. Morais, R. Mendoa, M. Dantas, H. Hekis, and R. Valentim, "Computer-aided detection system for lung cancer in computed tomography scans: Review and future prospects," *BioMedical Engineering OnLine*, vol. 13, p. 41, 2014.
16. S. Hawkins, H. Wang, Y. Liu, A. Garcia, O. Stringfield, H. Krewer, Q. Li, D. Cherezov, R. A. Gatenby, Y. Balagurunathan, D. Goldgof, M. B. Schabath, L. Hall, and R. J. Gillies, "Predicting malignant nodules from screening ct scans," *Journal of Thoracic Oncology*, vol. 11, no. 12, pp. 2120–2128, 2016.
17. M. S. AL-TARAWNEH, "Lung cancer detection using image processing techniques," *Leonardo Electronic Journal of Practices and Technologies*, pp. 147–158, June 2012.
18. O. Ronneberger, P. Fischer, and T. Brox, "U-net: Convolutional networks for biomedical image segmentation," *CoRR*, vol. abs/1505.04597, 2015.

Design and Analysis of CNN approach for the Lung Cancer Detection Using Image Processing

¹Dr. Sheetanshu Rajoriya, ²Mr. Pramod Kumar Sharma,
¹Supervisor, ²Ph.D Scholar, Sunrise University, Alwar

ABSTRACT

In this paper, we propose a versatile profound area learning system for partner picture qualities with hereditary data from tumors. Our methodology outfits the capability of the space variation strategy for genomic imaging to measure picture qualities dependent on comparative information territories. This is refined by making it simpler to learn tumor imaging with bigger datasets from comparable spaces to decrease dependence on enormous volumes of infection explicit datasets for genomics research imaging.

Also, our proposed structure considers the extraction of extra visual tumor descriptors to give conceptual picture portrayals to relationship with hereditary articulations. It exploits the present status of the workmanship in perceiving picture objects to give picture attributes that encode inconspicuous varieties in the phenotypic qualities of the tumor. The evaluation of these attributes is encouraged by the utilization of space variation procedure.

We assessed our proposed profound space variation learning structure by contrasting and present status of-the-workmanship in: (I) tumor histopathology picture arrangement and; (ii) the level of picture genomics affiliations, contrast and human-created tumor picture descriptors.

KEYWORDS: CNN, ML, Lung Cancer, Image Processing, Deep Learning.

I. INTRODUCTION

This theory tends to this test in the field of medical picture investigation, where our methodology offers extra imaging functionalities with an area variation procedure to encode the portrayal of the extra tumor aggregate. This theory depicts exploration to address two key speculations: Can space transformation encourage medical picture investigation and treatment applications? Assuming this is the case, is the area variation ready to infer visual tumor descriptors that produce more grounded relationship with hereditary data?

The image is the communication mode most used in different fields such as medical field, research field, industry, military area, etc. The significant picture move will happen over an unstable Internet organization. Along these lines, there is a requirement for satisfactory security for the picture to keep an unapproved individual from getting to significant data. The benefit of the picture is that it covers more media information and necessities security [4]. Cryptography is a sort of picture security strategy; It offers the protected technique for sending and putting away the picture over the Internet. Security is the primary worry of any framework to keep up the uprightness, privacy and genuineness of the picture. In the event that cryptography is the compelling strategy, you likewise face the security issue if the grayscale information is more

various [1].

The most well-known encryption components are AES, DES, 3DES, RSA, and SEA and The IDEA these systems are broadly utilized for pictures, recordings, and so on.

Modern cryptography can be classified into two types:-

A. Symmetric key cryptography

In the form of cryptography, there is only one key as the "private" key is used to encrypt and decrypt the data between the sender and the recipient.

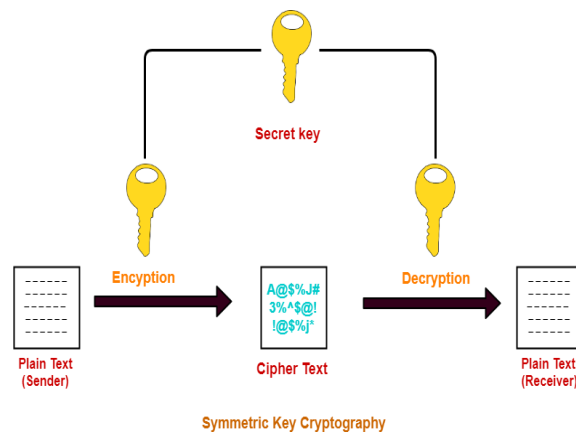


Fig 1: Symmetric key cryptography

B. Asymmetric key cryptography

In this form of cryptography, there are 2 types of keys: the public key and the private key and both are used in the Encryption and decryption process. The public key is available to all the world.

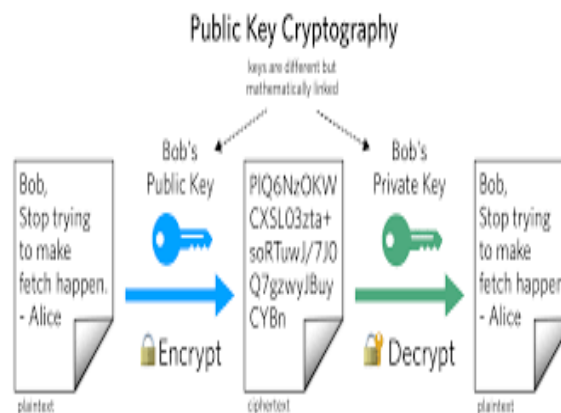


Fig 2: Asymmetric key cryptography

II. DIGITAL IMAGE PROCESSING (DIP)

DIP stands for the processing of snap shots, which might be virtual in nature through a digital computer. Its miles the purchase and processing of an picture. We are able to carry out a big quantity of duties, inclusive of enhancing pictorial statistics for human belief, image processing for independent gadget utility, efficient storage and transmission. Under human perception, the following applications of Digital Image Processing are: medical imaging, remote sensing, weather forecasting, atmospheric study and astronomy. Under machine vision, the following applications of Digital Image processing are: automated inspection, boundary information and video sequencing processing.

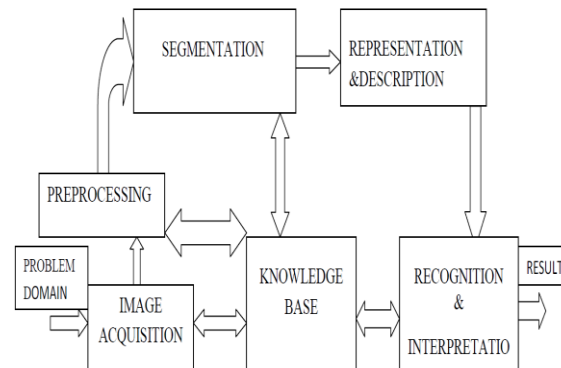


Fig 3 : Fundamental Steps in Image Processing

There are following steps in digital image processing:

1. **Image acquisition:** An imaging sensor and the ability to digitize the sign produced through the sensor.
2. **Image pre-processing:** Enhances the image quality, filtering, contrast enhancement.
3. **Image segmentation:** To partition an input image into its components or objects.
4. **Image representation:** Convert the input data to a format suitable for computer processing.
5. **Image description:** Extract functionalities that give rise to interesting quantitative information or basic functionalities to differentiate one object class from another.
6. **Image recognition and Interpretation:** Assign a label to an object based on the information provided by its descriptors and assign a meaning to a set of recognized objects.
7. **Knowledge base:** Contributes to efficient processing as well as module cooperation.

III. IMAGE DIGITALIZATION

Each matrix element represented by one of the finite set of discrete values. An image should be represented by infinite number of points. Each such image point may contain one of the infinitely

many possible intensity/colour values needing infinite number of bits. Obviously, such a representation is not possible by any digital computer.

IV. IMAGE-GENOMICS

Imaging hereditary qualities is a quickly arising field that is opening up another scene of disclosure in medication and neuroscience. The field is a mixture exertion that combines techniques and disclosures in both imaging and hereditary qualities; its capacity has as of late taken a quantum jump for various reasons. To begin with, numerous gatherings overall are checking a great many people with primary and useful attractive reverberation imaging (MRI). Tests are currently huge enough to find and confirm impacts of explicit qualities on the mind [1]. Second, voxel-wise genomic strategies are arising that search each area in a mind picture for measurable impacts of qualities [4]. These methodologies recognize cognizant anatomical examples of quality impacts in 3D. Replication endeavors would then be able to zero in on chosen cerebrum quantifies that show guarantee in primer investigations.

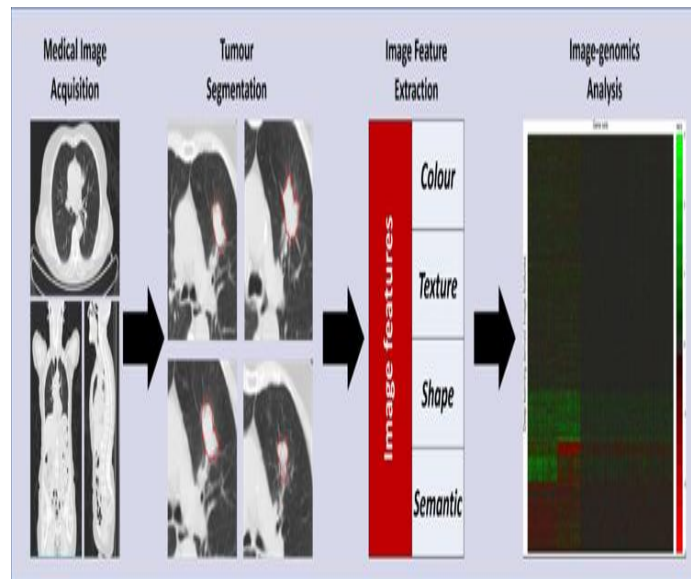


Fig 4: Associating image features with gene expression profiles using current image-genomic approach

V. ANALYSIS OF DOMAIN ADAPTATION FACILITATED MEDICAL IMAGE

This section portrays our proposed space variation encouraged medical picture examination framework. The space transformation conspire expects to beat the dependence on enormous volumes of commented on datasets for learning tumor picture portrayals and to improve medical picture examination with respect to tumor picture arrangement. We assess our technique by contrasting with the customary scratch-prepared CNNs for tumor order task. Our outcomes demonstrate that area transformation encourages the preparation cycle of CNNs and show improved forecast correct nesses for the tumor picture characterization undertakings where

preparing datasets are restricted.

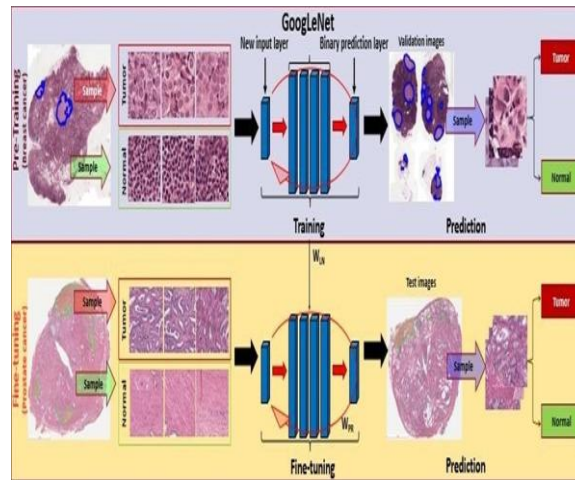


Fig 5: Patch-level tumour detection proposed model overview

VI. DEEP IMAGE-GENOMICS

This section subtleties our proposed profound space variation learning structure for picture genomics examination. Our business locales the momentum hole in picture genomics examination to separate extra, integral picture includes that encode complex conceptual portrayals of tumor phenotypic attributes for picture genomics affiliation. We assess our proposed picture genomics system with the present status-of-the-craftsmanship in picture genomics investigation to look at the levels of relationship between picture highlights and the tumor hereditary data. Our outcomes recommend that the proposed system gives stable picture highlights to encode tumor phenotypic attributes. Results further show that the extricated picture highlights offers more grounded relationship to tumor fundamental hereditary data and can possibly distinguish imaging substitutes for tumor prognostic biomarkers.

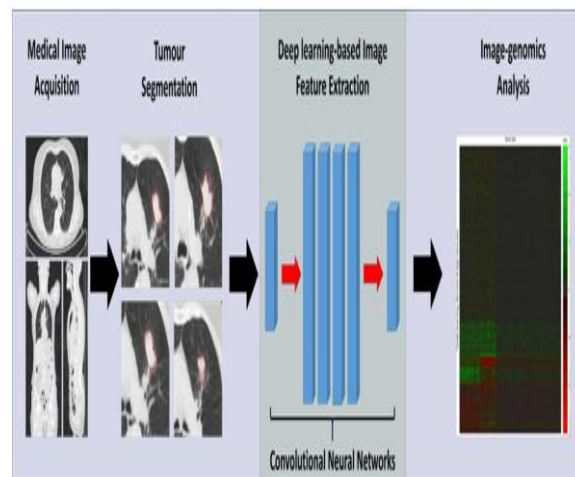


Fig 6: The proposed deep image-genomics framework

VII. CONCLUSION

In this Paper, we introduced novel profound space variation learning structure for picture genomics examination to improve picture genomics affiliation. Our proposed structure stressed the work of area transformation of profound learning in picture genomics exploration to offer extra profound picture includes that encode conceptual picture portrayals of inconspicuous variety in tumor medical pictures. Our space variation approach diminishes the reliance on enormous volumes of commented on medical picture dataset for profound learning models to gain proficiency with the tumor picture portrayal.

Our outcomes exhibited that area variation strategy encourages the learning of picture portrayals of irregularities in medical pictures by broadening or refining existing information from comparable areas. The measurement of such picture includes henceforth improves the exactness of tumor picture order assignments, contrasted with customary methodologies where profound taking in models were prepared without any preparation on restricted volumes of area explicit datasets. Our outcomes likewise showed that the proposed system offers extra profound picture highlights to encode theoretical portrayal of tumor phenotypic qualities which display more grounded relationship to tolerant explicit hereditary data, contrasted with human-created picture highlights.

REFERENCES

1. F. S. Collins and H. Varmus, "A new initiative on precision medicine," *New England Journal of Medicine*, vol. 372, pp. 793-795, 2015.
2. P. L. Bedard, A. R. Hansen, M. J. Ratain, and L. L. Siu, "Tumour heterogeneity in the clinic," *Nature*, vol. 501, p. 355, 2013.
3. C. A. Karlo, P. L. Di Paolo, J. Chaim, A. A. Hakimi, I. Ostrovnaya, P. Russo, et al., "Radiogenomics of clear cell renal cell carcinoma: associations between CT imaging features and mutations," *Radiology*, vol. 270, pp. 464- 471, 2014.
4. P. M. Evans, "Anatomical imaging for radiotherapy," *Physics in Medicine & Biology*, vol. 53, p. R151, 2008.
5. M. Rutman and M. D. Kuo, "Radiogenomics: creating a link between molecular diagnostics and diagnostic imaging," *European journal of radiology*, vol. 70, pp. 232-241, 2009.
6. H. Z. Sailem and C. Bakal, "Identification of medically predictive metagenes that encode components of a network coupling cell shape to transcription by image-omics," *Genome research*, vol. 27, pp. 196-207, 2017.
7. A. Friedman, A. Letai, D. E. Fisher, and K. T. Flaherty, "Precision medicine for cancer with next-generation functional diagnostics," *Nature Reviews Cancer*, vol. 15, p. 747, 2015.
8. J. L. Jameson and D. L. Longo, "Precision medicine—personalized, problematic, and promising," *Obstetrical & Gynecological Survey*, vol. 70, pp. 612-614, 2015.
9. M. Schwaederle, M. Zhao, J. J. Lee, A. M. Eggermont, R. L. Schilsky, J. Mendelsohn, et al., "Impact of precision medicine in diverse cancers: a meta- analysis of phase II medical trials," *Journal of medical oncology*, vol. 33, pp. 3817-3825, 2015.

10. D. A. Fisher, L. L. Zullig, S. C. Grambow, D. H. Abbott, R. S. Sandler, R.H. Fletcher, et al., "Determinants of medical system delay in the diagnosis of colorectal cancer within the Veteran Affairs Health System," *Digestive diseases and sciences*, vol. 55, pp. 1434-1441, 2010.
11. L. Stanton and P. R. Snider, "Coping with a breast cancer diagnosis: A prospective study," *Health Psychology*, vol. 12, p. 16,1993.
12. P. Lambin, E. Rios-Velazquez, R. Leijenaar, S. Carvalho, R. G. vanStiphout, P. Granton, et al., "Radiomics: extracting more information from medical images using advanced feature analysis," *European journal of cancer*, vol. 48, pp. 441-446, 2012.
13. D. L. Hill, P. G. Batchelor, M. Holden, and D. J. Hawkes, "Medical image registration," *Physics in medicine & biology*, vol. 46, p. R1,2001.
14. K. Doi, "Computer-aided diagnosis in medical imaging: historical review, current status and future potential," *Computerized medical imaging and graphics*, vol. 31, pp. 198-211, 2007.
15. E.-J. Yeoh, M. E. Ross, S. A. Shurtleff, W. K. Williams, D. Patel, R. Mahfouz, et al., "Classification, subtype discovery, and prediction of outcome in pediatric acute lymphoblastic leukemia by geneexpression profiling," *Cancer cell*, vol. 1, pp. 133-143, 2002.
16. L. J. Van't Veer, H. Dai, M. J. Van De Vijver, Y. D. He, A. A. Hart, M. Mao, et al., "Gene expression profiling predicts medical outcome of breast cancer," *nature*, vol. 415, p. 530,2002.
17. C. R. King, "Patterns of prostate cancer biopsy grading: trends andmedical implications," *International journal of cancer*, vol. 90, pp. 305-311,2000.
18. B. L. Baisden, H. Kahane, and J. I. Epstein, "Perineural invasion, mucinous fibroplasia, and glomerulations: diagnostic features of limited cancer on prostate needle biopsy," *The American journal of surgical pathology*, vol. 23, p. 918, 1999.
19. B. Bain, "Bone marrow biopsy morbidity and mortality: 2002data," *International Journal of Laboratory Hematology*, vol. 26, pp. 315-318, 2004.



Source details

International Journal of Control and Automation

Scopus coverage years: from 2010 to 2014, from 2018 to 2020

(coverage discontinued in Scopus)

Publisher: Science and Engineering Research Support Society

ISSN: 2005-4297

Subject area: [Engineering: Control and Systems Engineering](#)

[View all documents >](#)

[Set document alert](#)

[Save to source list](#) [Journal Homepage](#)

CiteScore 2019

0.2



SJR 2019

0.102



SNIP 2019

0.257

